Spectroscopic and Kinetic Analyses Reveal the Pyridoxal 5′-Phosphate Binding Mode and the Catalytic Features of *Treponema denticola* Cystalysin[†]

Mariarita Bertoldi,[‡] Barbara Cellini,[‡] Tim Clausen,[§] and Carla Borri Voltattorni*[,‡]

Dipartimento di Scienze Neurologiche e della Visione, Sezione di Chimica Biologica, Facoltà di Medicina e Chirurgia, Università degli Studi di Verona, Strada Le Grazie, 8, 37134 Verona, Italy, and Max-Planck Institut für Biochemie, Abteilung Strukturforschung, 82152 Martinsried, Germany

ABSTRACT: To obtain insight into the functional properties of *Treponema denticola* cystalysin, we have analyzed the pH- and ligand-induced spectral transitions, the pH dependence of the kinetic parameters, and the substrate specificity of the purified enzyme. The absorption spectrum of cystalysin has maxima at 418 and 320 nm. The 320 nm band increases at high pH, while the 418 nm band decreases; the apparent pK_{spec} of this spectral transition is about 8.4. Cystalysin emitted fluorescence at 367 and 504 nm upon excitation at 320 and 418 nm, respectively. The pH profile for the 367 nm emission intensity increases above a single pK of ~8.4. On this basis, the 418 and 320 nm absorbances have been attributed to the ketoenamine and substituted aldamine, respectively. The pH dependence of both log k_{cat} and log k_{cat}/K_m for α,β-elimination reaction indicates that a single ionizing group with a pK value of ~6.6 must be unprotonated to achieve maximum velocity. This implies that cystalysin is more catalytically competent in alkaline solution where a remarkable portion of its coenzyme exists as inactive aldamine structure. Binding of substrates or substrate analogues to the enzyme over the pH range 6−9.5 converts both the 418 and 320 nm bands into an absorbing band at 429 nm, assigned to the external aldimine in the ketoenamine form. All these data suggest that the equilibrium from the inactive aldamine form of the coenzyme shifts to the active ketoenamine form on substrate binding. In addition, reinvestigation of the substrate spectrum of α,β-elimination indicates that cystalysin is a cyst(e)ine C−S lyase rather than a cysteine desulfhydrase as claimed previously.

Treponema denticola belongs to the group of oral spirochetes which are known to be implicated in the etiology of periodontal diseases. In vitro studies revealed that this oral pathogen produces a large number of virulence factors contributing to disease progression (*1*, *2*). Cystalysin is a pyridoxal 5′-phosphate (PLP) Cβ-Sγ lyase isolated from *T. denticola* that catalyzes the cleavage of L-cysteine to pyruvate, ammonia and H_2S (*3*, *4*). It is also reported that the enzyme possesses hemolytic and hemoxidative activities, probably due to its ability to generate the toxic substance H_2S (*4−6*). Thus, cystalysin represents a new class of PLP-dependent virulence factors.

An outline of the desulfhydration catalyzed by cystalysin, showing the principal intermediates, is given in Scheme 1. This mechanism is based on that of other enzymes that catalyze PLP-dependent α,β-elimination reactions (*7*). Upon binding of the substrate cysteine, the Michaelis complex **I**

is rapidly converted to the external aldimine **II**, followed by α-proton abstraction to yield an α-carbanion stabilized as the quinonoid intermediate **III**. Subsequent elimination of H_2S generates the PLP derivative of aminoacrylate **IV**. Protonation of the aminoacrylate and reverse transaldimination then form iminopropionate and regenerate the enzyme-bound PLP. Hydrolysis of iminopropionate to pyruvate and ammonia presumably occurs outside the active site. In addition to L-cysteine, *T. denticola* cystalysin accommodates β-chloroalanine, cysteine methyl ester, S-ethylcysteine, and S-methylcysteine as substrates for β-elimination reactions (*5*).

Recently, the spatial structure of recombinant *T. denticola* cystalysin and of the cystalysin-L-aminoethoxyvinglycine complex has been determined by X-ray crystallography (*8*). The enzyme exists as a homodimer with 399 amino acids per subunit. Similarly to most PLP−enzymes of the L-aspartate aminotransferase family, each cystalysin monomer folds into two domains: (i) the large domain, consisting of residues 42−288 and carrying the PLP cofactor covalently bound to Lys 238, and (ii) the small domain, which is assembled by the two terminal regions of the polypeptide chain, namely, by residues 1−47 from the N-terminal end and residues 288−399 from the C-terminal part. On the basis of the enzyme active site architecture, a catalytic mechanism

* To whom correspondence should be addressed. Tel.: +39-045-8027-175. Fax: +39-045-8027-170. E-mail: carla.borrivoltattorni@ univr.it.
‡ Università degli Studi di Verona.
§ Max-Planck Institut für Biochemie.
¹ Abbreviations: PLP, pyridoxal 5′-phosphate; PMP, pyridoxamine 5′-phosphate; C-DES, cysteine/cystine desulfhydrase.

Scheme 1:   Proposed Mechanism of α,β-elimination for Cystalysin
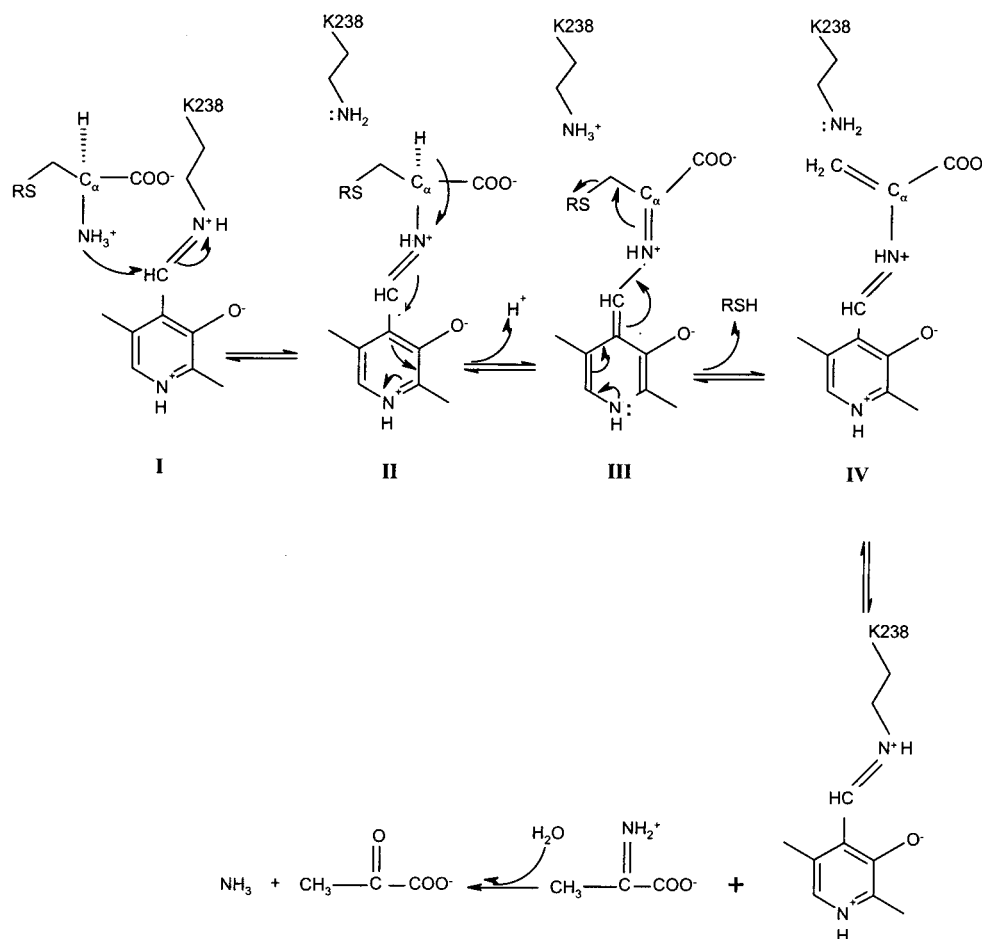
has been also proposed (*8*). The three-dimensional structures of other Cβ−Sγ lyases have been also solved, and plausible mechanisms of action have been proposed (*9−12*). However, there is a general absence of information in the literature on the spectroscopic features of bound PLP C−S lyases and on the identification of their intermediates along the catalytic pathway.

In the present study, we report a rapid and efficient two-step purification procedure by which large amounts of the recombinant protein can be obtained. We have examined the structure of the bound coenzyme and its involvement in catalysis by analyzing the pH dependence of the spectral properties and of the steady state kinetic parameters of this highly purified enzyme. Changes of the spectroscopic properties of cystalysin as a consequence of binding of substrates and substrate analogues are also described. In addition, a reinvestigation of the reaction of cystalysin with several sulfur-containing amino acids has revealed a desulfhydrase efficiency for disulfur amino acids higher than that for L-cysteine.

EXPERIMENTAL PROCEDURES

Chemicals. PLP, L-cystathionine, L-cystine, L-serine, β-chloro-L-alanine, O-acetyl-L-serine, glycine, L-homoserine, L-methionine, phenylhydrazine hydrochloride, NADH, pyruvate, rabbit muscle L-lactic dehydrogenase, and isopropyl β-D-thiogalactoside were from Sigma. L-Cysteine was either from Sigma or Fluka. L-Djenkolic acid was a generous gift

of Dr. Dorothea Kessler (University of Heidelberg). All other chemicals were the highest grade commercially available. Bis-Tris-propane at 20 mM final concentration was used over the pH range 6−10, and the ionic strength was maintained constant by addition of KCl.

Enzyme Preparation. Cystalysin from *Treponema denticola* was expressed in *E. coli* as described previously (*8*) with slight modifications. In brief, *E. coli* DH5α transformed with the plasmid pLC67 was grown in 1 l of Luria broth at 37 °C. Induction was performed after 6 h with 0.1 mM isopropyl-β-D-thiogalactopyranoside for 15 h at 30 °C. From the above-mentioned culture the cells were pelleted and resuspended in 10 mM potassium phosphate buffer, pH 8.2. Lysozyme was then added to a concentration of 100 μg/mL followed by a 15 min incubation at room temperature. After a freeze−thaw, leupeptin (0.5 μg/mL) and pepstatin (0.7 μg/mL) were added, and the suspension was then centrifuged at 30 000g for 30 min at 4 °C. The cleared lysate was diluted to approximately 20 mg/mL, adjusted to pH 7.6, and loaded on a DEAE-Sepharose FF XK 26/20 column previously equilibrated with 10 mM potassium phosphate buffer, pH 7.6, and washed with the same buffer. A linear gradient was then inserted (0−100%, 120 min) with the same buffer containing 100 mM potassium phosphate. Active fractions were pooled and brought to 90% saturation with solid $(NH_4)_2SO_4$. The precipitate was collected by centrifugation and dissolved in about 3 mL of 20 mM potassium phosphate buffer, pH 7.4. The solution was applied to a Superdex 200

XK 26/60 column equilibrated with the same buffer. The enzyme, eluted as a symmetrical peak, was concentrated to about 1 mL by Centriprep (Amicon) and stored at −70 °C without apparent loss of activity for at least 1 month. The enzyme concentration was determined from the absorbance of the peptide backbone at 205 nm, as described by Scopes (13). Utilizing this method, the apparent molar absorption coefficient at 281 nm was 12.77×10^4 M^{-1} cm^{-1}. This value is 0.7% greater than that reported previously (8). PLP content of holocystalysin was determined by releasing the coenzyme in 0.1 M NaOH and by using $\epsilon_M = 6600$ M^{-1} cm^{-1} at 388 nm.

Enzyme Assays. Pyruvate formation during the reaction of cystalysin with various substrates was assayed by coupling the pyruvate produced to the NADH-dependent lactate dehydrogenase-catalyzed reaction. Assays were performed at 25 °C on a Jasco V-550 spectrophotometer at 340 nm. A typical reaction mixture contained 2 mM L-cysteine, 300 μM NADH, 200 μg lactic acid dehydrogenase in 20 mM potassium phosphate buffer, pH 7.4, in a final volume of 250 μL. The reaction was initiated by addition of 1−10 μg of cystalysin. One unit of activity was defined as the amount of enzyme needed to convert 1 nmol of NADH to NAD$^+$/min at 25 °C. A molar extinction coefficient of 6220 M^{-1} cm^{-1} for NADH at 340 nm was used. Determination of the kinetic parameters for the reactions catalyzed by cystalysin was performed by measuring the initial velocities by the assay described above at varying concentration of each substrate.

Preparation and Reconstitution of Apoenzyme. The coenzyme PLP was removed as a phenylhydrazone. To a solution containing about 2 mg of holoenzyme in 3 mL of 20 mM potassium phosphate buffer, pH 7.4, was added phenylhydrazine hydrochloride to a final concentration of 40 mM. After 1 h at 25 °C, phenylhydrazone was removed either by extensive conventional dialysis or by repeated forced dialysis and redilution (six cycles) through Centricon microconcentrators (Amicon). Kinetics of reconstitution of holoenzyme was monitored by conventional spectrophotometry measurements: PLP was added to a final concentration of 50 μM to both the apoenzyme (14 μM) and reference cuvette, and spectra were taken at various times. The apparent equilibrium constant for dissociation of PLP from cystalysin, K_d, was determined by measuring enzymatic activity of the apoenzyme (10 nM) in the presence of PLP at a concentration ranging from 0.05 and 100 nM.

Spectrophotometric Measurements. Absorption measurements were made with a Jasco V-550 spectrophotometer. The enzyme solution was drawn through a 0.2 μm filter to reduce light scattering from the small amount of precipitate. Fluorescence spectra were taken with a FP750 Jasco spectrofluorometer using 5 nm bandwidths on both sides at a protein concentration varying from 0.07 to 14 μM. Spectra of blanks, i.e., of samples containing all components except cystalysin, were taken immediately prior to measurements of samples containing protein. Blank spectra were subtracted from spectra of samples containing enzyme. CD spectra were obtained with a Jasco J-710 spectropolarimeter with a thermostatically controlled cell compartment at 25 °C. For near-UV and visible wavelengths, protein concentrations between 0.6 and 1 mg/mL were used in a cuvette with a 1 cm path length. Routinely, four spectra were recorded at a scan speed of 50 nm/min with a bandwidth of 2 nm and averaged automatically except where indicated.

Data Analysis. Initial velocity data obtained by varying substrate concentrations were fitted to a hyperbolic curve using eq 1:

$$\frac{v}{E_t} = \frac{k_{cat}S}{(K_m + S)} \tag{1}$$

In the case of deviations from hyperbolic kinetics, initial velocity data obtained by varying substrate concentrations were fitted to a nonhyperbolic curve to eq 2 that takes into account substrate inhibition, i.e., binding of a second molecule of substrate to the ES complex to form an inactive ternary complex SES (*14*):

$$\frac{v}{E_t} = \frac{k_{cat}}{1 + \dfrac{K_m}{S} + \dfrac{S}{K_i}} \tag{2}$$

where E_t is the total enzyme concentration, k_{cat} the maximum velocity, S the substrate concentration, K_m the apparent Michaelis−Menten constant, and K_i the dissociation constant for the inhibitory SES ternary complex.

The K_d value of the enzyme-coenzyme complex was obtained using a tight-binding hypothesis according to eq 3:

$$Y = Y_{max} \frac{[E]_t + [PLP]_t + K_d - \sqrt{([E]_t + [PLP]_t + K_d)^2 - 4[E]_t[PLP]_t}}{2[E]_t} \tag{3}$$

where $[E]_t$ and $[PLP]_t$ represent the total concentrations of cystalysin dimer and PLP, respectively, Y refers to the enzymatic activity change at the PLP concentration [PLP], and Y_{max} refers to the enzymatic activity when all enzyme molecules are complexed with coenzyme.

Fractional changes in fluorescence emission for glycine and L-methionine or in dichroic signal for L-homoserine used to determine the dissociation constants for these substrate analogues were fitted using eq 4:

$$Y = \frac{A}{K_D + A} \tag{4}$$

where Y is the fractional change at any concentration of A, A is the analogue concentration, and K_D is the dissociation constant for the analogue.

Absorbances data recorded at 418 nm and at 320 nm were fitted to eqs 5 and 6, respectively:

$$A = \frac{A_1 - A_2}{1 + 10^{pH - pk_{spec}}} + A_2 \tag{5}$$

$$A = \frac{A_1 - A_2}{1 + 10^{pk_{spec} - pH}} + A_2 \tag{6}$$

where A_1 and A_2 are the higher and lower absorbances limits at a particular wavelength, respectively. Emission fluorescence intensity data recorded at 367 nm (exc. 320 nm) were fitted to eq 6. In this case, A_1 and A_2 are the higher and lower emission intensity limits, respectively.

Table 1: Summary of Purification of *Treponema Denticola* Cystalysin Expressed in *E. Coli*

step	vol (ml)	protein (mg)	total activity (units)	specific activity (units/mg)	yield (%)	purification (fold)
cleared lysate	70	1680	212 800	127	100	—
DEAE-FF	50	49.8	118 000	2369	55	18.6
Sephadex200	25	27	100 000	3703	47	29.1

The values for log k_{cat} and log k_{cat}/K_m as a function of pH were fitted to the appropriate equations:

$$\log Y = \log \frac{C}{1 + \dfrac{H}{K_A}} \qquad (7)$$

$$\log Y = \log \frac{C}{1 + \dfrac{H}{K_A} + \dfrac{K_B}{H}} \qquad (8)$$

here K_A and K_B represent the ionization constants for enzyme or reactant functional group, Y is the value of the parameter observed as a function of pH, and C is the pH-independent value of Y.

All data were fitted to the above equations using the Sigma Plot (SPSS) program.

RESULTS

Purification Procedure. The results of a typical purification procedure are summarized in Table 1. The method outlined in this paper offers a rapid, easy-to-perform and reproducible way for obtaining purified recombinant cystalysin. The final step gives a 29-fold purification with 47% recovery of the original activity, and the preparation has a specific activity of 3700 U/mg. SDS—PAGE analysis of the recombinant enzyme shows a single band (data not shown).

Spectral Properties of Recombinant Cystalysin. Purified cystalysin is bright yellow in color due to the presence of the PLP cofactor bound to the enzyme. At pH 7.4, the native enzyme exhibits absorption maxima at 281 and 418 nm with a A_{281}/A_{418} ratio of 10. In addition, a small shoulder at about 320 nm could be observed. The stoichiometric ratio of PLP to enzyme was estimated by measuring the A_{388} of the free cofactor, which was released upon incubation of the native holoenzyme at alkaline conditions (0.1 M NaOH). By this method, the PLP content of 2 mol/mol of the physiological dimer was found, as observed previously (8). The 418 nm absorption band is bleached by addition of NaBH$_4$, while an absorbance increase at 335 nm occurs. The spectral changes are consistent with reduction of an aldimine linkage between PLP and a lysine residue (K238). The absorption spectra of cystalysin in the pH range between 6 and 9.7 are shown in Figure 1. The relative intensities of the absorbances at 418 and 320 nm depend on pH: the 320 nm band increases with pH, while the 418 nm band decreases. The spectra do not show an isosbestic point suggesting the presence of multiple species. When we fitted the data to curves with one, two or three ionizations, we found that they fit best to a model with one ionization: the pK_{spec} values obtained were 8.37 ± 0.07 and 8.35 ± 0.12 for the absorbance at 418 and 320 nm, respectively (Figure 1, inset).
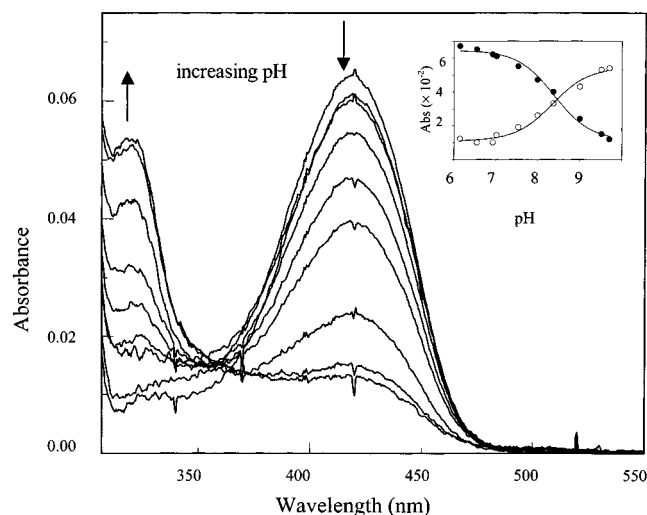

FIGURE 1: pH dependence of the UV—visible spectra of cystalysin. Spectra of cystalysin (4.6 μM) were acquired in 20 mM Bis-Tris-propane at pH 6.14, 6.55, 6.93, 7.54, 8.00, 8.37, 9.00, 9.51, and 9.70. The inset shows the pH dependence of the absorbances at 418 (●) and 320 nm (○). The solide lines represent the theoretical curves according to eqs 5 and 6: 418 nm (p$K_{spec} = 8.37 \pm 0.07$, eq 5) and 320 nm (p$K_{spec} = 8.35 \pm 0.12$, eq 6).
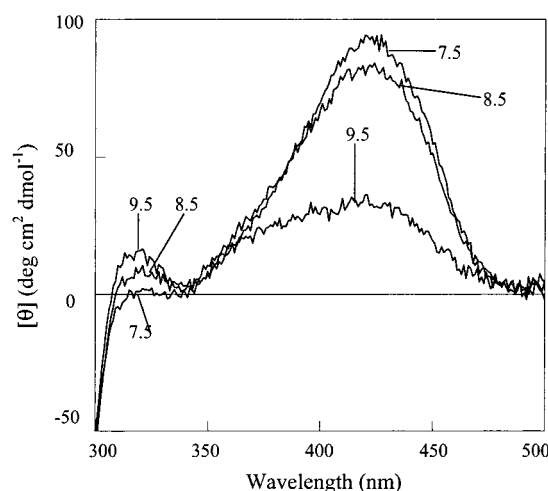

FIGURE 2: CD spectra of cystalysin at various pH. CD spectra of 8.1 μM cystalysin in 20 mM Bis-Tris-propane at pH values indicated.

CD spectra were recorded for cystalysin at three pH values. As shown in Figure 2, the CD spectrum displays two positive dichroic bands at 422 and 340 nm whose intensity changes with pH, such that the 422 nm signal decreases, while the 340 nm signal increases with increasing pH. At three pH values, the enzyme displays optical activity values of about 76 mdeg/A_{418} and about 9 mdeg/A_{320}, suggesting a different chiral environment for the two coenzyme bands.

The fluorescence emission spectrum of cystalysin at pH 7.4 when excited at 281 nm exhibits two maxima at 337 nm and around 500 nm (Figure 3A and inset). Like in other PLP—enzymes (15—18), in addition to the intrinsic trypto-phan fluorescence (λ_{max} 337 nm), an energy transfer band ($\lambda_{max} \sim 500$ nm) is generated as a result of the proximity of tryptophan residue(s) to the protonated internal Schiff base of the active site PLP. The ratio of F_{337}/F_{500} is about 86. Excitation of cystalysin at 418 nm results in an extremely faint emission band at 504 nm, typical of the emission of
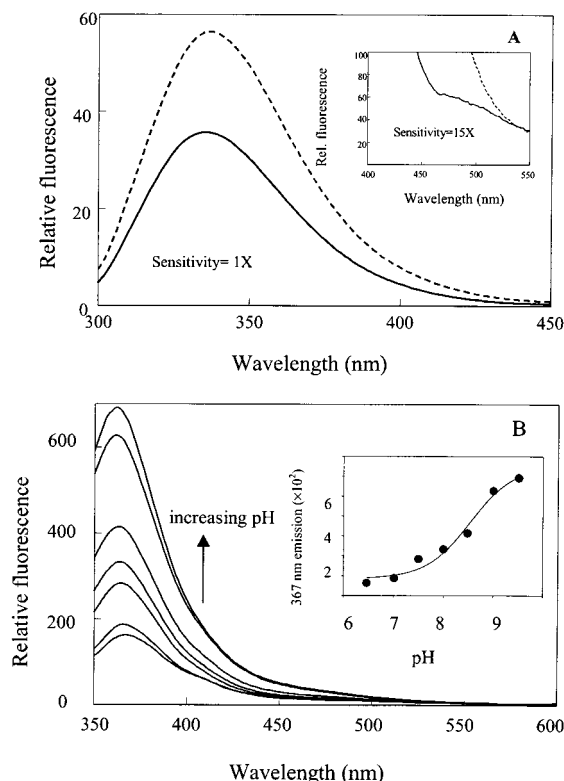
FIGURE 3: Fluorescence emission spectra of cystalysin. (A) Fluorescence emission spectra (excitation was at 281 nm) of (—) holoenzyme and (---) apoenzyme in 20 mM potassium phosphate buffer, pH 7.4, at a concentration of 70 nM. Inset: Exc. at 281 nm. Fluorescence emission spectra of holoenzyme and apoenzyme in the 400−500 nm range at the indicated sensitivity. Symbols are the same as above. (B) fluorescence emission spectra of holoenzyme (14 μM) in 20 mM Bis-Tris-propane at pH 6.47, 7.02, 7.50, 8.00, 8.48, 9.00, and 9.51 upon excitation at 320 nm. The inset shows the pH dependence of the 367 nm emission intensity (exc. 320 nm). The solid line represents the theoretical curve from a fit of the data using eq 6.

Schiff bases of PLP in an aqueous environment at neutral pH (*19−21*). Moreover, cystalysin emitted at 367 nm upon excitation at 320 nm. When the fluorescence was monitored at 504 and 367 nm, the excitation spectra exhibited, in addition to a maximum at 275 nm, maxima at 418 and 320 nm, respectively (data not shown). Emission fluorescence intensity at 367 nm increases with increasing pH (Figure 3B). As shown in the inset of Figure 3B, the pH profile for the 367 nm emission intensity increases above a single pK of 8.48 ± 0.1.

Properties of the Apoenzyme. The phenylhydrazine-treated cystalysin had no residual activity, whereas the reconstituted enzyme completely recovered its original activity. The apoenzyme does not exhibit either absorbance and dichroic bands in the visible region or PLP emission fluorescence. However, the emission spectrum of apoenzyme is not identical to that of holoenzyme, when excited at 281 nm. The emission band is 2 nm blue-shifted and has an intensity 1.5-fold higher than that of the holoenzyme (Figure 3A).

On reconstitution of holoenzyme, occurring within the time required for manual mixing of PLP and apoenzyme, the absorbance, fluorescence and dichroic features of the co-enzyme-associated bands are restored to an intensity comparable to that of the starting material. From titration analysis of the apoenzyme with PLP the data for enzyme activity
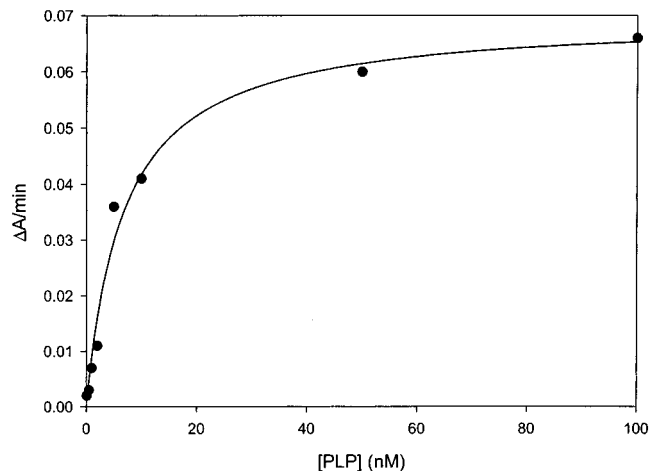

FIGURE 4: Titration of apo−cystalysin with PLP. Apoenzyme (10 nM) was incubated with 2 mM L-cysteine in 20 mM potassium phosphate buffer, pH 7.4, at various PLP concentrations. Pyruvate production was measured by the spectrophotometric assay described under the Experimental Procedures section. Changes in initial velocity were plotted as a function of [PLP] in the sample solution. The line was theoretical from a fit to eq 3.

versus PLP concentration fitted to eq 3 yielded a K_d value for the PLP−cystalysin complex equal to 6.6 ± 1.0 nM, consistent with the occurrence of a very tight interaction between the coenzyme and the apoprotein (Figure 4).
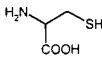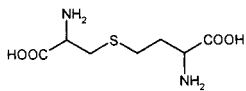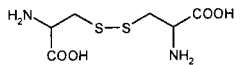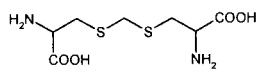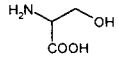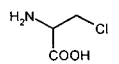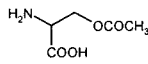
Steady-State Kinetics Studies. To investigate the substrate preferences of cystalysin, we examined several sulfur and non-sulfur containing amino acids for pyruvate formation. Their kinetic parameters were determined in 20 mM potassium phosphate buffer, pH 7.4, at 25 °C and are reported in Table 2. The enzyme has a strong preference for L-djenkolic acid over other amino acids, having the highest k_{cat}/K_m. It should be noted that when the reaction with L-cystine or L-djenkolic acid was run until complete depletion of the substrate, 2 mol of pyruvate was finally yielded per mol of disulfide amino acid employed. This stoichiometry indicates further enzymatic (and possibly also spontaneous) reactions of the primary elimination product (see Discussion). Both D-cysteine and D-cystine behave as poor substrates: at a concentration of 2 mM, the initial rate is 0.48 and 0.18 nmol pyruvate/min/nmol enzyme, respectively.

The purified cystalysin obeys Michaelis−Menten kinetics with all substrates examined except for L-cysteine, for which substrate inhibition was observed. L-Cysteine used was either from Sigma or Fluka and was maintained under reducing conditions by adding dithiothreitol. It was checked that the inhibition was not due to the dithiothreitol added to the reaction mixture. Initial velocity data at low and high L-cysteine concentrations fit well using eq 2 (describing substrate inhibition, *14*) to a nonhyperbolic curve to yield K_m and K_i values of 0.63 ± 0.11 and 8.3 ± 1.5 mM, respectively (Figure 5).

Glycine, methionine, and homoserine do not act as substrates. They inhibit, even if to different extents, the desulfhydrase activity (data not shown), thus providing evidence for their binding to the enzyme (see below).

pH Dependence of Kinetic Parameters for Cystalysin. The pH dependence of the kinetic parameters for cystalysin toward β-L-chloroalanine and L-serine was determined, and the results are shown in Figure 6A and B. Log k_{cat} decreases

Table 2: Kinetic Parameters for Substrates in 20 mM Potassium Phosphate Buffer, pH 7.4, at 25 °C

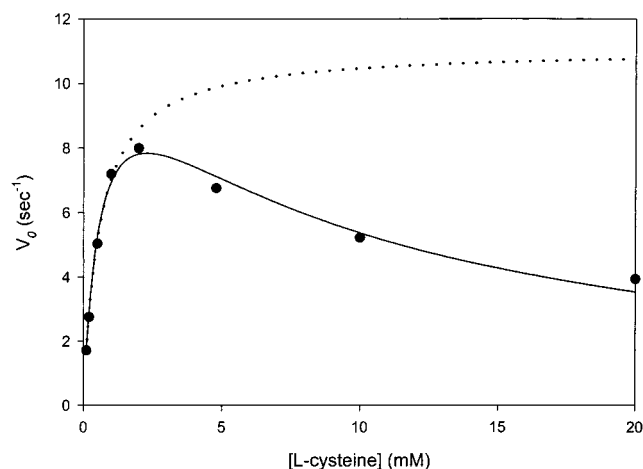|	K_m (mM)	k_{cat} (s^{-1})	k_{cat}/K_m (M^{-1}s^{-1})	structure
L-cysteine	0.63 ± 0.11	11.4 ± 0.3	18095 ± 3135	
L-cystathionine	1.38 ± 0.2	13.03 ± 0.7	9442 ± 1458	
L-cystine[a]	0.68 ± 0.05	21.1 ± 0.3	31029 ± 1876	
L-djenkolic acid	0.99 ± 0.15	72.2 ± 6.7	72929 ± 12863	
L-serine	6.92 ± 1.15	0.36 ± 0.02	52 ± 9.1	
β-chloro-L-alanine	1.21 ± 0.15	59.9 ± 2.3	49504 ± 6419	
O-acetyl-L-serine	1.6 ± 0.2	63.3 ± 3.0	39562 ± 5283	

[a] Measured at pH 8.4.

FIGURE 5: Substrate inhibition of cystalysin by L-cysteine. 0.1 μM enzyme was incubated with increasing concentrations of L-cysteine, and pyruvate production was measured by the spectrophotometric assay described under the Experimental Procedures section. Changes in initial velocity were plotted as a function of L-cysteine concentration. (—) A fit of all the data to eq 2; (····) a fit of the data at low L-cysteine concentration to eq 1.

below a pK of 6.67 ± 0.06 and 6.52 ± 0.03 for β-L-chloroalanine and L-serine, respectively. The variation with pH of log k_{cat}/K_m gives rise to a bell-shaped profile for β-L-chloroalanine: fitting of the data to eq 8 yielded pK values of 6.55 ± 0.08 and 8.66 ± 0.07. Log k_{cat}/K_m profile for L-serine exhibits a single pK value of 6.56 ± 0.07. Unfortunately, assays at pH values above pH 8.8 are not reliable because of the spontaneous racemization of L-serine (22).

Absorption and CD Spectral Changes of Cystalysin with Substrates and Substrate Analogues. Amino acid substrates and substrate analogues are used in an attempt to stop the desulfhydrase cystalysin-catalyzed reaction at specific points along the reaction pathway in order to identify reaction intermediates. Except for L-serine, the rate of α,β-elimination for the substrates tested (Table 2) is very high, and reaction of the enzyme with these substrates cannot be studied by conventional spectroscopy.

Addition of L-serine to cystalysin at pH 7.4 produces an immediate shift from 418 to 429 nm (Figure 7A). During the steady-state conditions, only an increase of the absorbance in the 340 nm region, due to the formation of pyruvate, is observed (data not shown). Similarly, upon mixing glycine with the enzyme at pH 7.4, a shift in the visible absorbance maximum from 418 to 429 nm was observed (Figure 7A). This shift is consistent with the conversion of internal to external aldimine. On the other hand, binding of L-methionine or L-homoserine at pH 7.4 to the enzyme results in mixtures of external aldimine and quinonoid species absorbing at 429 and 508 nm, respectively (Figure 7A). L-Serine or glycine added to the enzyme at pH 8.8 or 9.5, respectively, leads to the disappearance of the 320 nm absorbance band and the concomitant appearance of an absorbing species at 429 nm (Figure 7A, inset).

To further characterize the enzyme-ligand intermediate complexes, we recorded CD spectra for cystalysin in the presence of saturating concentrations of L-serine, glycine, L-methionine, and L-homoserine. As shown in Figure 7B, after addition of L-serine or glycine to the enzyme, a negative
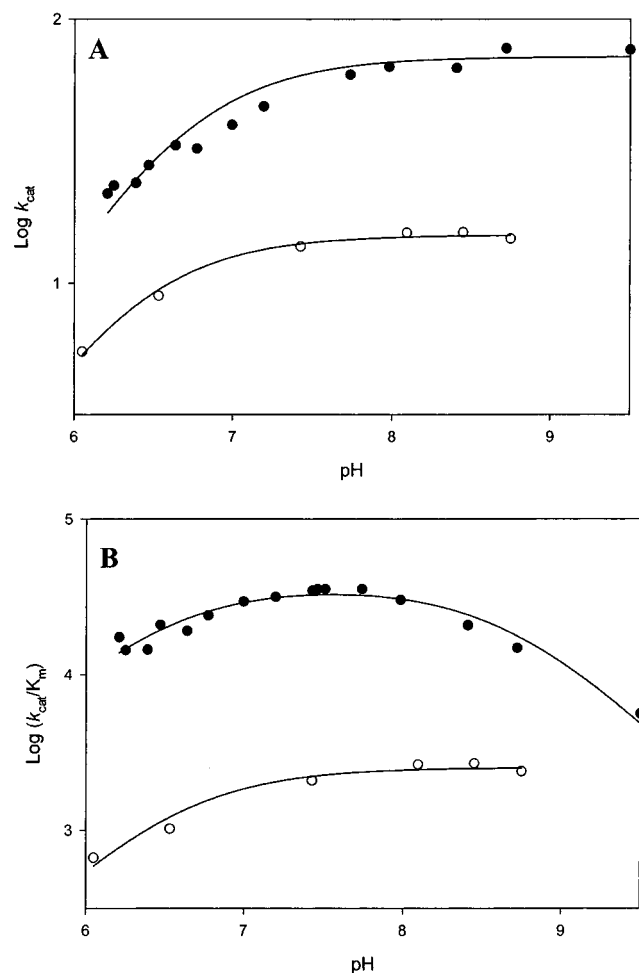
FIGURE 6: pH dependence of the kinetic parameters for cystalysin reaction with β-L-chloroalanine and L-serine. (A) log k_{cat} profile and (B) log k_{cat}/K_m profile for β-L-chloroalanine ($\bullet$) and L-serine ($\bigcirc$). The points shown are experimentally determined values, while the curves are from fits to the data using eq 7 for log k_{cat} for both substrates and for log k_{cat}/K_m for L-serine, and eq 8 for k_{cat}/K_m for β-L-chloroalanine.

dichroic signal at about 460 nm appears, while after addition of L-methionine or L-homoserine, a decrease in the intensity of the 422 nm dichroic band and no dichroic signal of the quinonoid were observed. In each case a modest change of the dichroic band at 340 nm seems to occur. Differences between the unliganded and liganded enzyme in the near-UV CD were also seen. The near-UV spectrum of cystalysin is characterized by negative dichroic bands in the aromatic region at 288−296 nm, which would indicate the asymmetry of certain aromatic amino acids, most probably associated with the active site (Figure 7B). Upon addition of ligands, a decrease of the original negative dichroic signals, more pronounced for L-serine and glycine, and the concomitant appearance of a positive band at 275 nm were observed (Figure 7B). Nevertheless, substrates or substrate analogues do not affect the far UV CD spectra of the enzyme (data not shown). The fractional changes in the intensity of the 422 nm dichroic band as a function of L-homoserine concentration were used to calculate the K_D for external Schiff base formation. The apparent K_D for L-homoserine is 265 ± 40 mM.

Fluorescence Spectra of Cystalysin in the Presence of Ligands. Excitation of cystalysin at 281 nm in the presence
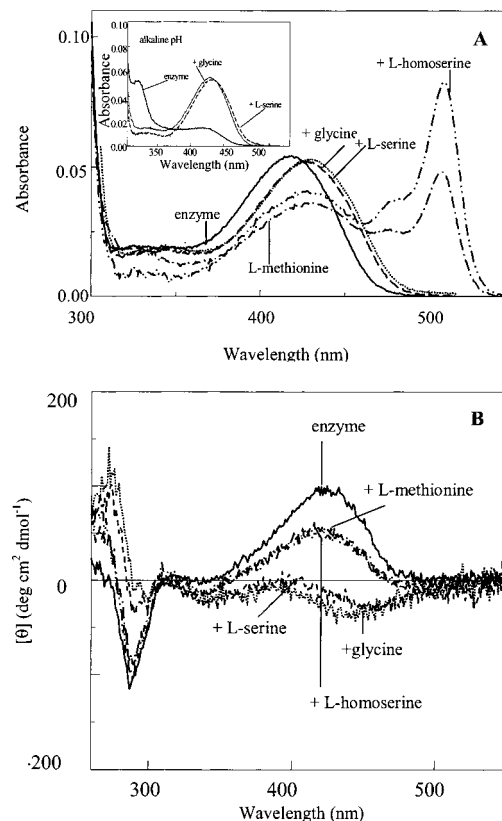

FIGURE 7: Absorption and CD spectra of cystalysin in the presence of L-serine, glycine, L-methionine, or L-homoserine. (A) Absorption spectra of enzyme (−) and in the presence of 50 mM L-serine (---), 20 mM glycine (···), 204 mM L-methionine (− · −), or 494 mM L-homoserine (− ·· −). In each case the enzyme concentration was 4.5 μM, and the buffer was 20 mM Bis-Tris-propane, pH 7.4. Inset: Absorption spectra at alkaline pH under the above experimental conditions. (B) CD spectra at pH 7.4, same as the absorption.

of L-serine, L-methionine, and glycine (at a concentration 4−10 times higher than K_m or K_D) at pH 7.4 shows a quenching of the tryptophan emission (23% for L-serine and glycine, 27% for L-methionine) shifted to 334 nm (Figure 8A). Furthermore, a long wavelength band develops which is of low intensity and very broad, ranging from <500 to about 550 nm for L-serine and glycine, and of remarkable intensity centered at 524 nm for L-methionine (Figure 8A, inset). Changes in PLP emission fluorescence of enzyme upon addition of these ligands have been also measured at pH 7.4. When the enzyme was excited at 429 nm in the presence of L-serine, glycine, or L-methionine, the emission spectrum exhibits an enhancement of the fluorescence emission at 504 nm, concomitant with a red shift from 504 to 518, 510, or 524 nm, respectively. The enhancement was about 3.9-fold for L-serine, 2.4-fold for L-methionine, and 1.8-fold for glycine (Figure 8B). Analysis of the enhancement data at 510 nm or at 524 nm as a function of glycine or L-methionine concentration yields apparent K_D values of 1.92 ± 0.09 and 44.3 ± 4.1 mM, respectively (data not shown). Fluorescence emission at 504 and 518 nm was also observed when the enzyme was mixed with L-serine at pH 8.8 or glycine at pH 9.5, respectively (Figure 8B, inset). Emission fluorescence measurements of the enzyme in the presence of L-homoserine following excitation either at 281 or 422 nm were prevented by the high intrinsic fluorescence of the analogue solution.
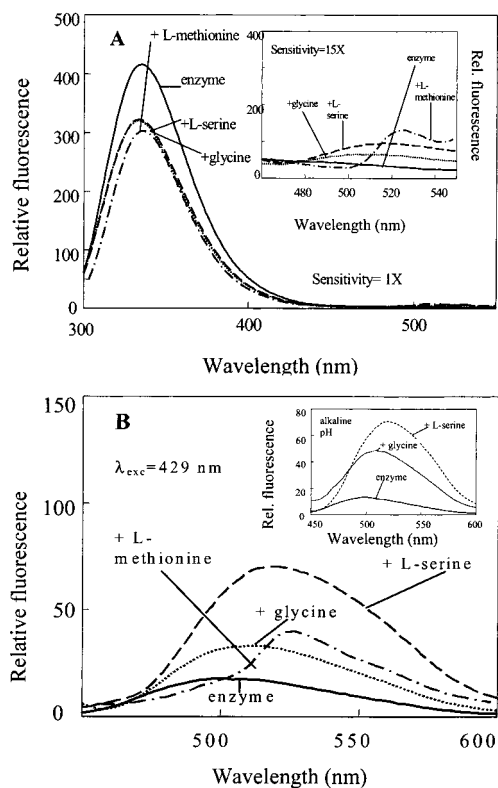
FIGURE 8: Fluorescence emission spectra of cystalysin in the presence of L-serine, glycine, or L-methionine. (A) Excitation was at 281 nm. Emission spectra of 1.04 μM enzyme (—) and in the presence of 50 mM L-serine (- - -), 20 mM glycine (···), or 204 mM L-methionine ($- \cdot -$). Instrument sensitivity was as indicated in the figure. Inset: Exc. at 281 nm. Fluorescence emission spectra of cystalysin alone and in the presence of the above ligands in the 460−550 nm range at the indicated sensitivity. Symbols are the same as above. (B) Excitation was at 429 nm. Emission spectra of the enzyme (4.9 μM) and in the presence of 50 mM L-serine, 20 mM glycine, or 204 mM L-methionine. Symbols are the same as those in panel A. Inset: Exc. at 429 nm. Emission spectra of the enzyme (4.9 μM) and in the presence of 50 mM L-serine or 20 mM glycine in 20 mM Bis-Tris-propane, pH 9.5. Symbols are the same as those above. In each case, except where indicated, the buffer was 20 mM Bis-Tris-propane, pH 7.4.

DISCUSSION

A high yield of recombinant cystalysin was obtained (27 mg of pure protein/liter of cell culture) using a two-step purification procedure. As evidenced by absorption, fluorescence, and CD features of the protein, cystalysin was isolated as the holoenzyme form which is characterized by a prominent absorption band at 418 nm, associated with a positive Cotton effect, and that gives rise to an emission maximum at 504 nm. In addition, the holoenzyme displays a species absorbing at about 320 nm associated with a CD band around 340 nm. The detectable emission with cystalysin, excited at 320 nm, is at 367 nm. The apo−cystalysin lacked completely either the absorption and CD bands in the visible range or the PLP emission fluorescence. When the intrinsic fluorescence emissions of holo and apo are compared, the results are consistent with a model in which a substantial fraction (at least 40%) of the tryptophan emission evident in apoenzyme is quenched in holoenzyme. This quenching is concomitant with the appearance of the 504 nm emission indicative of energy transfer from tryptophanyl residue(s) to the internal Schiff base. Interaction

Scheme 2: Structures of the Ketoenamine Form (**I**), the Enolimine Form (**II**), the Pyridine Nitrogen Deprotonated Form (**III**), and the Substituted Aldamine Form (**IV**)
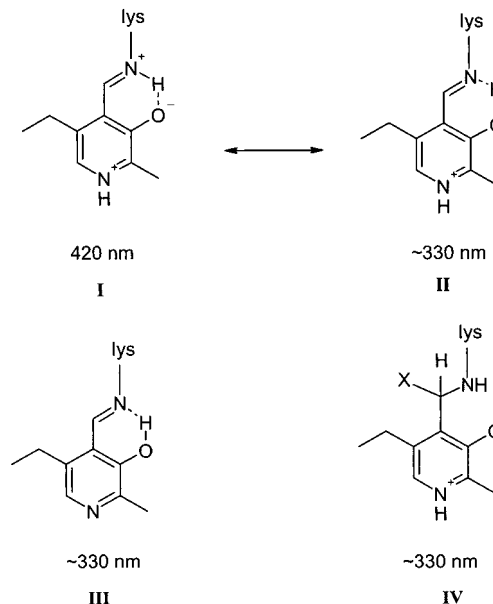
between apoenzyme and the coenzyme is extremely tight, being characterized by a K_d value of 6.6 nM. This value is 75 and 750 times smaller than those determined for the *Arabidopsis thaliana* and *E.coli* cystathionine β-lyases, respectively (*23, 24*). Crystallographic data indicate a tight binding of PLP in C-DES (9) and NifS (10) and a weak binding in MalY (11).

The spectral changes of cystalysin as a function of pH reveal that the 418 nm band decreases at higher pH, while the 320 nm band increases. On excitation of the 320 nm band, the emission intensity at 367 nm increases with increasing pH. While the absorbing species at 418 nm can be attributed to a protonated aldimine, the assignment to the 320 nm species is more problematic. Structures which could account for an increase in the 330 nm region at high pH have been postulated to arise from the conversion from the ketoenamine to the enolimine tautomer (Scheme 2, **I** → **II**), from deprotonation of the pyridine nitrogen N1 (Scheme 2, **III**) or from formation of an adduct upon the addition of a deprotonated nucleophilic or a hydroxy group to the imine double bond (Scheme 2, **IV**). Deprotonation of the imine nitrogen gives rise to a 360 nm maximum, which is not evident in the spectra of cystalysin. The three-dimensional structure of cystalysin reveals that an active site aspartate residue (D203) is located near the pyridinium nitrogen of PLP (8) and is thought to increase the pK value of the nitrogen. Stabilization of the positively charge pyridine nitrogen is a conserved feature in the aspartate aminotransferase family of PLP−enzymes and has been shown to contribute to the electron sink character of the conjugated pyridine system. In fact, it has been estimated that the binuclear D222−pyridine nitrogen base has a pK value of ~13 in native aspartate aminotransferase (*25*). Therefore, it is difficult to consider the deprotonation of this pyridine nitrogen of cystalysin-bound PLP. It remains to establish which structure, the enolimine tautomer or the substituted aldamine, can account for the 320 nm absorption of cystalysin. These two species can be distinguished by fluorescence

spectroscopy. It is known that a substituted aldamine (Scheme 2, **IV**) gives a maximum emission wavelength at around 390 nm when excited at around 330, whereas the enolimine structure (Scheme 2, **II**) emits fluorescence with a maximum intensity at around 510 nm (*26, 27*). The fluorescence spectra of cystalysin showed an emission band at 367 nm with excitation at 320 nm (Figure 3B). This observation, which rules out the attribution of the 320 nm absorption of cystalysin to the enolimine tautomer structure, is consistent with the assignment of this form to a substituted aldamine. It should be noted that the 320 nm maximal absorbance of cystalysin is 5−10 nm lower than that reported for an aldamine structure. On the other hand, the above attribution is in apparent contrast with our results. When cystalysin was treated with phenylhydrazine, the absorption bands at 418 and 320 nm were lost, and the resultant apoenzyme lacked the fluorescence bands at 504 and 367 nm. Moreover, at alkaline pH, where the 320 nm species is pronounced, binding of L-serine or glycine to cystalysin causes the disappearance of both the 320 and 418 nm bands with the concomitant appearance of an absorbance band at 429 nm. Excitation at 429 nm results in an enhancement of the emission intensity at around 510−518 nm. Again, cystalysin is catalytically more competent at alkaline pH, where the 320 nm species increases at the expense of the 418 nm species. These data indicate that cystalysin must change at alkaline pH its coenzyme structure to an active form to metabolize a substrate. It follows that binding of substrates and substrate analogues shifts the equilibrium from the inactive substituted aldamine to the active ketoenamine structure. The resultant ketoenamine is favorable for transaldimination with the substrate amino group, a prerequisite for subsequent catalysis. At present, the mechanism involved in this transition is elusive. A similar activation of the coenzyme at an early step of the catalytic cycle has been already described for tryptophanase. It was postulated that the electrostatic interaction of the coenzyme with the ligand promotes the removal of the nucleophilic group (or the hydroxide ion) from the tetrahedral adduct (*28*).
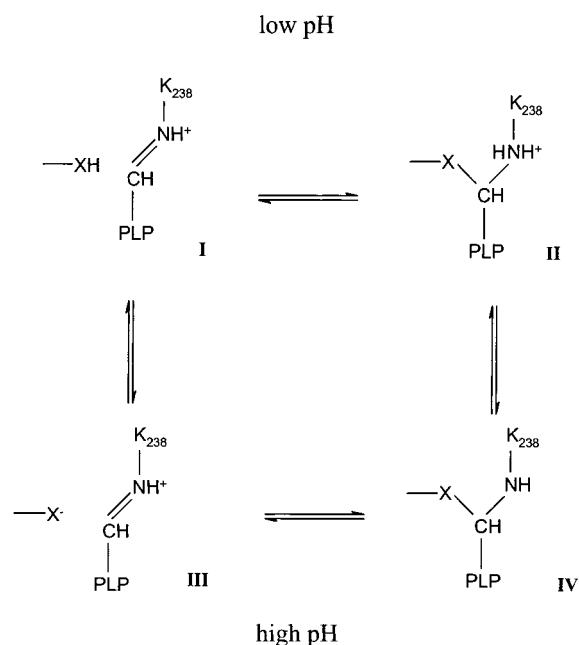
Another possibility to be considered for the reason behind the shift in equilibrium between the 418 and 320 nm absorbance bands on ligand binding is the ligand-induced conformational change of the enzyme. The effects of any amino acid tested on the CD and fluorescence spectra of cystalysin consist, even to a different extent, in quenching of intrinsic tryptophan fluorescence, enhancement, and red shift of the long wavelength PLP emission, change in the dissymmetry of bound cofactor and aromatic amino acids possibly located near the active site. All together, these data can be interpreted in terms of local perturbations, as changes in the orientation of the PLP and in the relative orientations of an aromatic residue(s) and of cofactor upon binding of amino acid, rather than gross conformational changes. Consistent with this view is the finding that in the crystal structure of L-aminoethoxyvinylglycine-liganded cystalysin the pyridine ring of PLP rotated slightly with respect to the position of the unliganded enzyme, while no major structural changes regarding domain movement have been observed (*8*). Nevertheless, it cannot be excluded that the modest ligand-induced alterations might contribute to the conversion of the aldamine structure of the coenzyme to the ketoenamine structure.

Some intermediates of the interaction between cystalysin and substrate analogues have been characterized with respect to their spectral properties using UV−visible, CD, and fluorescence spectroscopy. Although glycine, L-methionine or L-homoserine bind to cystalysin in an unproductive mode, there is a difference in their interaction with the enzyme. Addition of glycine results in formation of external Schiff base, while L-methionine or L-homoserine give equilibrating mixtures of external aldimine and quinonoid species. This implies that glycine stops the reaction at the step of the external aldimine, whereas L-methionine or L-homoserine stop at the quinonoid intermediate. Quinonoid species have been already detected in other β-eliminases, as tyrosine phenol-lyase (*29*) and tryptophanase (*30*). These results can be explained by a model in which a compound with zero side-chain carbon is unable to maintain the scissile bond parallel to the aldimine p orbitals, thus preventing the subsequent hydrogen abstraction. A similar proposal has been advanced by Sun et al. (*31*) to explain how the reactivity of dialkylglycine decarboxylase toward substrates depends on their side chain size. Unlike the above-mentioned ligands, L-serine binds productively to cystalysin, and a quinonoid intermediate is expected to be generated along the α,β-elimination pathway (**III**, Scheme 1). The fact that it is not detected could probably mean that the rate of quinonoid complex formation is lower or equal to that its decomposition rate. Interestingly, unlike several other β-elimination or β-replacement PLP−enzyme systems (*32−36*), this enzyme does not seem to generate the α-aminoacrylate Schiff base of PLP as detectable species. We intend to clarify this aspect by performing stopped-flow analysis of the interaction of the enzyme with other substrates.

It should be also pointed out that, although the addition of L-serine, glycine, L-methionine or L-homoserine to cystalysin causes a shift from 418 to 429 nm, it results in distinctly different changes of their coenzyme dichroic bands (Figure 7A and B). This suggests that binding of L-serine or glycine causes changes in the orientation of the coenzyme, with respect to the neighboring residues, different from those caused by the binding of L-methionine or L-homoserine. Accordingly, differences between L-serine-or glycine-enzyme complex and L-methionine- or L-homoserine-enzyme complex were also observed in the near-UV CD signals.

Titration of enzyme-bound coenzyme absorbance or fluorescence over the pH range of 6−9.7 are consistent with a deprotonation event with a pK value of ∼8.4 (inset of Figures 1 and 3). However, examination of the absorbance titration curves indicates that at pH values much lower than the apparent pK some 320 nm material is still present and that at pH values higher than pK some 418 nm absorbing species remains. This observation, together with the lack of an isosbestic point, suggests the involvement of multiple absorbing species, ruling out a pH-dependent interconversion of only two species. On the basis of observations that the 320 nm absorption species is most probably the substituted aldamine (see above), we propose a model shown in Scheme 3. The scheme involves XH−**I** and X⁻−**III** ketoenamine forms absorbing at 418 nm and protonated **II** and unprotonated **IV** substituted aldamine species absorbing at 320 nm. At pH values less than pK, **I** and **II** will be present, whereas **III** and **IV** represent the forms at pH values greater than the pK. A group (XH) was assumed to form an adduct

Scheme 3: Structures of the Coenzyme in Cystalysin

low pH

$$K_{238}$$
$$NH^+$$
—XH   CH
PLP   **I**

$$K_{238}$$
HNH$^+$
—X   CH
PLP   **II**

$$K_{238}$$
$$NH^+$$
—X$^-$ CH
PLP   **III**

$$K_{238}$$
NH
—X   CH
PLP   **IV**

high pH

with the imino group of the Schiff base, and the deprotonated form X$^-$ is considered to be more favorable for forming this adduct. Two candidates for nucleophilic attack to C4′ of the coenzyme are the residue Y64* (a residue from the neighboring subunit) and a water molecule, which are within 3.75 and 3.86 Å of the imine bond, respectively (8). Other residues are located (Y123, H206) more than 4 Å from C4′. Aldamine formation governs the two equilibria between **I** and **II** as well as between **III** and **IV**. Instead, a deprotonation/protonation event is responsible for the equilibria between species spectroscopically indistinguishable, i.e., **I** to **III** and **II** to **IV**. Accordingly, the spectral pK of 8.4 would not reflect the ionization of K238 in the internal aldimine linkage. It could rather reflect either the ionization of XH which shifts the equilibria toward **IV** or another enzymic group whose ionization would influence the equilibrium between the species absorbing at 418 and 320 nm.

The results for the desulfhydrase reaction either with β-L-chloroalanine or L-serine indicate that a single ionizing group with a pK value of about 6.6 must be unprotonated to achieve maximum velocity. This same ionizing group is observed in the k_{cat}/K_m profiles, and thus, it can be concluded that this group is involved in catalysis but not in binding. The k_{cat}/K_m profiles for β-L-chloroalanine exhibit a second ionizing residue, with a pK value of ∼8.6 that must be protonated for reaction. Because the pK value of the α-amino group of β-L-chloroalanine is 8.6 (measured by direct titration), the observed pK value could reflect ionization of the substrate. Since it was not possible to perform experiments with L-serine at pH higher than 8.8, we could not to verify if the pK of the α-amino group of L-serine (9, 27) was present in the k_{cat}/K_m profile. The assignment of the pK of 6.6 to an enzymic group of the enzyme rises some problems. One might speculate that this pK is largely associated with ionization of K238, for which a catalytic role has been already advanced (8). If this were true, one would find the pK of 6.6 in the spectral titration, considering that the k_{cat}/K_m pH rate profile reflects free enzyme (where K238 is in internal aldimine linkage) and free substrate. However, on

the basis of the proposed model for the structures of the coenzyme in cystalysin (Scheme 3), the observed 418 → 320 nm transition does not reveal the protonation state of the iminic nitrogen; rather, it reflects the structural change of the internal Schiff base. The separation of the spectral and the kinetic pK (8.4 vs 6.6, respectively) is not unprecedented for PLP—enzymes in that it has been already observed in a mutant of 1-aminocyclopropane-1-carboxylate synthase (37). However, it can be also considered that the pK of 6.6 could be attributed to an enzymic group other than K238 involved in catalysis. Whatever the enzymic group with pK of 6.6 could be, the catalytic mechanism of cystalysin appears to require a single catalytic base. Instead, the pH dependence of the kinetic parameters for tyrosine phenol-lyase (38) and tryptophan indole-lyase (39) provides support for a mechanism requiring two catalytic bases. One of these abstracts the proton from the α-position of the substrate to form a quinonoid intermediate, and the second, acting in concert with proton transfer from the first group, facilitates the elimination of the carbon leaving group (phenol or indole). From a mechanistic standpoint, the elimination of a carbon leaving group in these C—C lyases implies that the enzymes have to activate the aromatic ring for elimination to take place. In contrast, this activation is not required for elimination of a heteroatom leaving group as in C—S lyases.

Like MalY and β-cystathionase, cystalysin belongs to the group of PLP-dependent Cβ—Sγ lyases. These enzymes catalyze the elimination of a Cβ-substituent to generate Cα,Cβ-unsaturated aldimine (generally the aminoacrylate—PLP Schiff base) leading to the formation of ammonium ion and pyruvate (Scheme 1). While MalY plays a role in the maltose regulon (11), β-cystathionine is involved in microbial and plant methionine biosynthesis (40), and cystalysin has a proposed role in virulence (4–6). MalY seems to prefer cystine over the β-cystathionase main substrate cystathionine; cystalysin seems to favor cysteine. Although the active site construction of these enzymes results in individual substrate preferences, the enzymes share basically the same organization of the active site key residues, as revealed by their recently solved three-dimensional structures (8, 11, 12). Thus, the conservation of a similar desulfhydrase reaction mechanism could be the consequence of divergent evolution.

To define the substrate specificity of cystalysin, we have examined the reaction of the enzyme with sulfur- and non-sulfur-containing amino acids as well as with disulfidic amino acids. The data shown in Table 2 indicate that cystalysin has a relatively broad substrate specificity. Structural elements of the substrate molecule playing a critical role in the catalytic efficiency of cystalysin catalyzed α,β-elimination are a second cysteinyl moiety (not necessarily linked through a disulfide bond) or a good leaving group (not necessarily in a sulfur-containing compound). Among the substrates investigated, only L-cysteine exhibits substrate inhibition. Likewise, C-DES from *Synechocystis* (41) and D-cysteine desulfhydrase (42) and β-cystathionase (43) from *E. coli* have been reported to show this peculiar behavior toward L-cysteine. The kinetics of cystalysin with L-cysteine is consistent with binding of a second, inhibitory molecule of L-cysteine to the enzyme—substrate complex. As a consequence, an unproductive ternary complex could be formed. However, the presence of a contaminant in L-cysteine, accounting for the inhibition, could not be excluded.

Our substrate specificity data concerning the desulfhydrase activity of cystalysin extend some previous findings (*5*) and clearly demonstrate that the catalytic efficiency of L-djenkolic acid and L-cystine is higher than that of L-cysteine. Among sulfur-containing amino acids, the lowest β-cleavage activity was obtained with L-cystathionine (Table 2). In light of these findings, cystalysin should more properly be considered as a cyst(e)ine C—S-lyase, rather than a cysteine desulfhydrase as claimed previously (*4, 5*). Recently, a L-cysteine/cystine C—S-lyase (named C-DES) from *Synechocystis*, which catalyzes the breakdown of L-cysteine to yield sulfide (assembled in ferredoxin) pyruvate and ammonia, was characterized by Leibrecht and Kessler (*44*). The enzyme displays a strong substrate preference for L-djenkolic and L-cystine over L-cysteine (*41*) and evidence for a C-DES-mediated cysteine persulfide generation during catalysis has been provided (*9, 41*). The formation of cysteine persulfide could represent an alternative pathway of S° production as compared with the sulfuration of an active site cysteine in NifS proteins (*45*). Interestingly, although cystalysin and C-DES, both belonging to fold type I, do not share sequence homology, they indeed display a desulfhydrase activity with similar substrate specificity. It should be also pointed out that cleavage by cystalysin of L-cystine and L-djenkolic acid, both harboring two L-cysteinyl moieties, finally yielded 2 mol of pyruvate per mol of substrate. Again, this is reminiscent of a stoichiometry already observed with the same substrates for C-DES from *Synechocystis* (*44*). On the basis of the crystal structure of cystalysin, the possibility that disulfuric compounds occupy both active sites with their respective cysteinyl moieties can be ruled out, since the distance between the two active sites in cystalysin is much too large. Like C-DES, the following mechanism involving generation of a substrate-derived persulfide can be anticipated for cystalysin, even if the spontaneous decomposition reaction of the primary reaction products was also feasible:
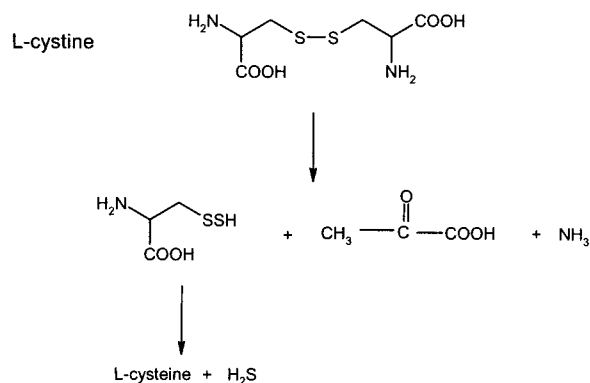
In conclusion, our results on spectroscopic analysis of the coenzyme and reaction intermediates as a function of pH together with those on the pH dependence of the kinetic parameters provide insight into the PLP binding mode in cystalysin. Evidence is also given for a ligand-induced activation of coenzyme, a prerequisite for catalysis, especially at alkaline pH. Further studies are required to identify either the nature of the group that is supposed to form an adduct with the PLP-Lys 238 aldimine or the mechanism of the activation process. Additionally, substrate specificity studies reveal that cystalysin displays catalytic features similar to those of C-DES: L-djenkolic acid and L-cystine are the preferred substrates and are completely decomposed to pyruvate and ammonia. It will be interesting to establish if the mechanism of action of cystalysin toward these substrates is similar to that of C-DES.

REFERENCES

1. Saglie, R., Newman M. G., Carranza, F. A., and Pattison, G. L. (1982) Bacterial invasion of gingiva in advanced periodontitis in humans, *J. Periodontol. 53*, 217−222.
2. Syed, S. A., Mäkinen, K. K., Mäkinen, P. L., Chen, C. Y., and Muhammed, Z. (1993) Proteolytic and oxidoreductase activity of *Treponema denticola* ATCC 35405 grown in an aerobic and anaerobic gaseous environment, *Res. Microbiol. 144*, 317−326.
3. Chu, L., and Holt, S. C. (1994) Purification and characterization of a 45 kDa hemolysin from *Treponema denticola* ATCC 35404, *Microbiol. Pathog. 16*, 197−212.
4. Chu, L., Ebersole, J. L., Kurzban, G. P., and Holt, S. C. (1997) Cystalysin, a 46-kilodalton cysteine desulfhydrase from *Treponema denticola*, with hemolytic and hemoxidative activities, *Infect. Immun. 65*, 3231−3238.
5. Kurzban, G. P., Chu, L., Ebersole, J. L., and Holt, S. C. (1999) Sulfhemoglobin formation in human erythrocytes by cystalysin, an L-cysteine desulfhydrase from *Treponema denticola*, *Oral Microbiol. Immunol. 14*, 153−164.
6. Chu, L., Ebersole, J. L., and Holt, S. C. (1999) Hemoxidation and binding of the 46-kDa cystalysin of *Treponema denticola* leads to a cysteine-dependent hemolysis of human erythrocytes, *Oral Microbiol. Immunol. 14*, 293−303.
7. Tai, C.-H., and Cook, P. F. (2001) Pyridoxal 5′-phosphate α, β-elimination reactions: mechanism of O-acetylserine sulfhydryl-ase, *Acc. Chem. Res. 34*, 29−59.
8. Krupka, H. I., Huber, R., Holt, S. C., and Clausen, T. (2000) Crystal structure of cystalysin from *Treponema denticola*: a pyridoxal 5′-phosphate-dependent protein acting as a haemolytic enzyme, *EMBO J. 19*, 3168−3178.
9. Clausen, T., Kaiser, J. T., Steegborn, C., Huber, R., and Kessler, D. (2000) Crystal structure of the cystine C—S lyase from *Synechocystis*: stabilization of cysteine persulfide for FeS cluster biosynthesis, *Proc. Natl. Acad. Sci. U.S.A. 97*, 3856−3861.
10. Kaiser, J. T., Clausen, T., Bourenkow, G. P., Bartunik, H.-D., Steinbacher, S., and Huber, R. (2000) Crystal structure of a NifS-like protein from *Thermatoga maritima*: implications for iron sulphur cluster assembly, *J. Mol. Biol. 297*, 451−464.
11. Clausen, T., Schlegel, A., Peist, R., Schneider, E., Steegborn, C., Chang, Y. S., Haase, A., Bourenkov, G., Bartunik., H. D., and Boose, W. (2000) X-ray structure of MalY from *Escherichia coli*: a pyridoxal 5′-phosphate-dependent enzyme acting as a modulator in mal gene expression, *EMBO J. 19*, 831−842.
12. Clausen, T., Huber, R., Laber, B., Pohlenz, H. D., and Messer-schmidt, A. (1996) Crystal structure of the pyridoxal 5′-phosphate dependent cystathionine beta-lyase from *Escherichia coli* at 1.83 Å, *J. Mol. Biol. 262*, 202−224.
13. Scopes, R. K. (1974) Measurement of protein by spectrophotom-etry at 205 nm, *Anal. Biochem. 59*, 277−282.
14. Copeland, R. A. (2000) Kinetics of single-substrate enzyme reactions, in *Enzymes*, 2nd ed., pp 137−141, John Wiley & Sons, Inc., New York.
15. Strambini, G. B., Cioni, P., Peracchi, A., and Mozzarelli, A. (1992) Characterization of tryptophan and coenzyme luminescence in tryptophan synthase from *Salmonella typhimurium*, *Biochemistry 31*, 7527−7534.
16. McClure, G. D., and Cook, P. F. (1994) Product binding to the α-carboxyl subsite results in a conformational change at the active site of O-acetylserine sulfhydrylase A: evidence from fluorescence spectroscopy, *Biochemistry 33*, 1674−1683.
17. Eisenstein, E., Yu, H. D., and Schwartz, P. D. (1994) Cooperative binding of the feedback modifiers isoleucine and valine to biosynthetic threonine deaminase from *Escherichia coli*, *J. Biol. Chem. 269*, 29423−29429.
18. Marceau, M., McFall, E., Lewis, S. D., and Shafer, J. A. (1988) D-serine dehydratase from *Escherichia coli*. DNA sequence and identification of catalytically inactive glycine to aspartic acid variants, *J. Biol. Chem. 263*, 16926−16933.
19. Arrio-Dupont, M. (1970) Fluorescence study of Schiff base of pyridoxal. Comparison with L-aspartate aminotransferase, *Photo-chem. Photobiol. 12*, 297−315.

20. Arrio-Dupont, M. (1971) The effect of solvent on the fluorescence of Schiff bases of pyridoxal 5′-phosphate, *Biochem. Biophys. Res. Commun.* 44, 653−659.

21. Shaltiel, S., and Cortijo, M. (1970) The mode of binding of pyridoxal 5′-phosphate in glycogen phosphorylase, *Biochem. Biophys. Res. Commun. 41*, 594−600.

22. Dawson, R. M. C., Elliott, D. C., Elliott, W. H., and Jones, K. M. (1986) Amino acids, amines, amides, peptides, and their derivatives, in *Data for biochemical research*, 3rd ed., pp 1−31, Oxford Science Publications, Oxford.

23. Burstein, E. A., Vedenkina, N. S., and Ivkova, M. N. (1973) Fluorescence and delocation of tryptophan residues in protein molecules, *Photochem. Photobiol. 18*, 263−279.

24. Ravanel, S., Job, D., and Douce, R. (1996) Purification and properties of cystathionine β-lyase from *Arabidopsis thaliana* overexpressed in *Escherichia coli*, *Biochem. J. 320*, 383−392.

25. Gloss, L. M., and Kirsch, J. F. (1995) Decreasing the basicity of the active site, Lys-258, of *Escherichia coli* of aspartate aminotransferase by replacement with γ-thialysine, *Biochemistry 34*, 3990−3998.

26. Hayashi, H., Mizuguchi, H., and Kagamiyama, H. (1993) Rat liver L-aromatic amino acid decarboxylase: spectroscopic and kinetic analysis of the coenzyme and reaction intermediates, *Biochemistry 32*, 812−818.

27. Ro, H. S., Hong, S. P., Seo, H. J., Yoshimura, T., Esaki, N., Soda, K., Kim, H. S., and Sung, M. H. (1996) Site-directed mutagenesis of the amino acid residues in beta-strand III [Val30-Val36] of D-amino acid aminotransferase of Bacillus sp. YM-1, *FEBS Lett. 398*, 141−145.

28. Ikushiro, H., Hayashi, H., Kawata, Y., and Kagamiyama, H. (1998) Analysis of the pH- and ligand-induced spectral transition of tryptophanase: activation of the coenzyme at the early steps of the catalytic cycle, *Biochemistry 37*, 3043−3052.

29. Kumagai, H., Utagawa, T., and Yamada, H. (1975) Studies on tyrosine phenol-lyase. Modification of essential histidyl residues by diethylpyrocarbonate,. *J. Biol. Chem. 250*, 1661−1667.

30. June, D. S., Suelter, C. H., and Dye, J. L. (1981) Equilibrium and kinetic study of interaction of amino acid inhibitors with tryptophanase: mechanism of quinonoid formation, *Biochemistry 20*, 2714−2719.

31. Sun, S. S., Zabinski, R. F., and Toney, M. D. (1998) Reactions of alternate substrates demonstrate stereoelectronic control of reactivity in dialkylglycine decarboxylase, *Biochemistry 37*, 3865−3875.

32. Phillips, R. S. (1991) Reaction of indole and analogues with amino acid complexes of *Escherichia coli* tryptophan indole-lyase: detection of a new reaction intermediate by rapid-scanning stopped-flow spectrophotometry, *Biochemistry 30*, 5927−34.

33. Phillips, R. S., Sundararaju, B., and Faleev, N. G. (2000) Proton transfer and carbon−carbon bond cleavage in the elimination of indole catalyzed by *Escherichia coli* tryptophan indole-lyase, *J. Am. Chem. Soc. 122*, 1008−1014.

34. Tai, C. H., Nalabolu, S. R., Jacobson, T. M., Minter, D. E., and Cook, P. F. (1993) Kinetic mechanisms of the A and B isozymes of O-acetylserine sulfhydrylase from *Salmonella typhimurium* LT-2 using the natural and alternative reactants, *Biochemistry 32*, 6433−6442.

35. Peracchi, A., Bettati, S., Mozzarelli, A., Rossi, G. L., Miles, E. W., and Dunn, M. F. (1996) Allosteric regulation of tryptophan synthase: effects of pH, temperature, and alpha-subunit ligands on the equilibrium distribution of pyridoxal 5′-phosphate-L-serine intermediates, *Biochemistry 35*, 1872−1880.

36. Jhee, K. H., Niks, D., McPhie, P., Dunn, M. F., and Miles, E. W. (2002) Yeast cystathionine beta-synthase reacts with L-allothreonine, a nonnatural substrate, and L-homocysteine to form a new amino acid, 3-methyl-L-cystathionine, *Biochemistry 41*, 1828−35.

37. Li, Y., Feng, L., and Kirsch, J. F. (1997) Kinetic and spectroscopic investigations of wild-type and mutant forms of apple 1-aminocyclopropane-1-carboxylate synthase, *Biochemistry 36*, 15477−15488.

38. Kiick, D. M., and Phillips, R. S. (1988) Mechanistic deductions from kinetic isotope effects and pH studies of pyridoxal phosphate carbon−carbon lyases: *Erwinai herbicola* and *Citrobacter freundii* tyrosine phenol-lyase, *Biochemistry 27*, 7333−7338.

39. Kiick, D. M., and Phillips, R. S. (1988) Mechanistic deductions from multiple and solvent deuterium isotope effects and pH studies of pyridoxal phosphate dependent carbon−carbon lyases: *Escherichia coli* tryptophan indole-lyase, *Biochemistry 27*, 7339−7344.

40. Giovannelli, J. (1990) in *Sulfur Nutrition and Sulfur Assimilation in Higher Plants* (Rennberg, H., Brunold, C., De Kok, L. J., and Stulen, I., Eds.) pp 33−48, SBP Academic, The Hague.

41. Lang, T., and Kessler, D. (1999) Evidence for cysteine persulfide as reaction product of L-cyst(e)ine C−S lyase (C-DES) from *Synechocystis*. Analyses using cystine analogues and recombinant C-DES, *J. Biol. Chem. 274*, 189−195.

42. Nagasawa, T., Ishii, T., Kumagai, H., and Yamada, H. (1985) D-cysteine desulfhydrase of *Escherichia coli*. Purification and characterization, *Eur. J. Biochem. 153*, 541−551.

43. Dwivedi, C. M., Ragin, R. C., and Uren, J. R. (1982) Cloning, purification, and characterization of β-cystathionase from *Escherichia coli*, *Biochemistry 21*, 3064−3069.

44. Leibrecht, I., and Kessler, D. (1997) A novel L-cysteine/cystine C−S-lyase directing [2Fe-2S] cluster formation of *Synechocystis* ferredoxin, *J. Biol. Chem. 272*, 10442−10447.

45. Zheng, L., White, R. H., Cash, V. L., and Dean, D. R. (1994) Mechanism for the desulfurization of L-cysteine catalyzed by the *nifS* gene product, *Biochemistry 33*, 4714−4720.